GEOPHYSICS, VOL. 34, NO. 1 (FEBRUARY 1969), P. 39–53, 9 FIGS., 1 TABLE

# THE EQUIVALENT SOURCE TECHNIQUE†

C. N. G. DAMPNEY*

The inherent ambiguity of potential field interpretation can be put to advantage. Bouguer anomaly measurements on an irregular grid and at a variety of elevations can be synthesized by an equivalent source of discrete point masses on a plane of arbitrary depth below the surface. By keeping the depth of the plane within certain limits relative to the station spacing, we can ensure that the synthesized field closely approximates the true gravity field in the region close to and above the terrain.

Once the equivalent source is obtained, the projection of the Bouguer anomaly onto a regularly gridded horizontal plane is easily done. In addition, the equivalent source can then be economically used to carry out vertical continuation. The technique is illustrated by a hypothetical example and a case history of a local gravity survey in precipitous topography.

## INTRODUCTION

A fundamental property of a potential field is the inherent ambiguity in determining its source from values of the field outside the source region. For instance, given the vertical anomalous gravitational field intensity, $g_z\ (x, y, z)$ over a horizontal plane, it is impossible to find the anomalous mass distribution uniquely.

Roy (1962) has discussed in detail the ambiguity of the relationship between $g_z\ (x, y, z)$ and $\sigma\ (\alpha, \beta, h)$ in the equation

$$g_z(x, y, z) = K \int_{-\infty}^{\infty} \int_{-\infty}^{\infty} \frac{\sigma(\alpha, \beta, h)(h - z)d\alpha d\beta}{\left\{(x - \alpha)^2 + (y - \beta)^2 + (z - h)^2\right\}^{3/2}} \tag{1.1}$$

where $\sigma\ (\alpha, \beta, h)$ is the surface contrast density distribution over the plane $z = h$, $K$ is the gravitational constant and the positive direction is down. We note that the depth $h$ of the apparent source may take any value.

To perform the inversion of equation (1.1) it is sufficient to have a complete knowledge of $g_z$ on a plane $z = z_1$ $z_1 < h$. Therefore a unique correspondence exists between the function $g_z\ (x, y, z = z_1)$ and $\sigma\ (x, y, h)$; and furthermore as a result of equation (1.1) any value of $g_z\ (x, y, z)$ for $z < h$ is similarly defined uniquely.

Thus we find a surface density contrast distribution on an arbitrary plane which synthesizes a known gravity field. It is then possible to calculate from gravity measurements at one height the gravity field at any other point in space. The projection and interpolation of the field from known points of measurement may thus be carried out.

By using the equivalent source $\sigma\ (\alpha, \beta, h)$ as an integral part of gravity field computations, two advantages result: (1) All available information contained in the measurements of $g_z\ (x, y, z)$ is used, and (2) we ensure the correct analytical gravity potential field behavior of the projected field values intrinsically as they are calculated from a gravitating equivalent source.

† Presented at the 37th Annual International SEG Meeting, Oklahoma City, Oklahoma, November 1, 1967. Manuscript received by the Editor December 4, 1967; revised manuscript received October 30, 1968.

* Dept of Geology, University of Tasmania, Australia; Contribution No. 187. Now with Geophysics Laboratories, University of Toronto, Canada.

## REVIEW

There are, in the literature, many data-processing techniques (e.g. Henderson, 1960; Bhattacharyya, 1965, 1966; Neidell, 1966; Sax 1966) which require data to be put on a gridded horizontal plane. In practice, however, points of measurement may be scattered horizontally and vertically over normal rough topography.

As Naudy and Neumann (1965) emphasize, the Bouguer anomaly must be regarded as being the vertical gravity field at points on the terrain due to the anomalous masses in the ground. The points are not situated on the geoid or some other reference surface. The observed values must not only be interpolated horizontally from their original coordinates of measurement, but be vertically projected onto the plane of the grid as well.

Projection of Bouguer anomalies onto a horizontal plane has received very little attention in the literature. Strakhov and Devitsyn (1965) and Grant and West (1965, p. 269) have proposed the only two solutions known to the author. In this paper we set up an equivalent source to represent and thereby interpolate and project the observed Bouguer anomaly values.

The idea of an equivalent layer has been exploited by Danes (1961) in gravity interpretation incorporating borehole data and recently by Bott (1967) to interpret magnetic anomaly profiles. This demonstrates that representing potential fields by an equivalent source may have many applications. In fact, as Zidarov (1965) showed, the idea can be applied to electrical fields and to the general Dirichlet-Neumann inverse problem as well as to gravity and magnetics.

Zidarov's (1960, 1965) papers give the general outline of representing potential fields by equivalent sources.

## THE EQUIVALENT SOURCE TECHNIQUE

From equation (1.1) we see that the anomalous gravitational field intensity $g_z\ (x,\ y,\ z)$ can be represented by or be synthesized from a continuous surface density contrast distribution $\sigma(\alpha,\beta,h)$ on any plane $z_1=h$. The equivalent source technique is based on approximating this continuous distribution by a series of discrete masses.

If we have $N$ data points, we can calculate the values of $N$ point masses at a suitable depth which will then constitute the equivalent source from the equations (using the principle of superposition).

$$\begin{aligned} g_1 &= a_{11}m_1 + a_{12}m_2 + \cdots \\ &\quad + a_{1k}m_k + \cdots + a_{1N}m_N \\ g_2 &= a_{21}m_1 + a_{22}m_2 + \cdots \\ &\quad + a_{2k}m_k + \cdots + a_{2N}m_N \\ &\cdots\cdots\cdots\cdots\cdots\cdots \\ g_i &= a_{i1}m_1 + a_{i2}m_2 + \cdots \\ &\quad + a_{ik}m_k + \cdots + a_{iN}m_N \\ &\cdots\cdots\cdots\cdots\cdots\cdots \\ g_N &= a_{N1}m_1 + a_{N2}m_2 + \cdots \\ &\quad + a_{Nk}m_k + \cdots + a_{NN}m_N, \end{aligned} \tag{3.1}$$

where the

$$a_{ik} = \frac{K(h - z_i)}{\left\{(x_i - \alpha_k)^2 + (y_i - \beta_k)^2 + (z_i - h)^2\right\}^{3/2}} \tag{3.2}$$

and $z=h$ is the horizontal plane containing the point masses $m_k$ at $(\alpha_k,\ \beta_k,\ h)$. The position of $g_i$ is $(x_i,\ y_i,\ z_i)$.

This can be written in matrix form

$$g = A\mathbf{m} \tag{3.3}$$

which represents $N$ simultaneous equations in $N$ unknowns and is thus solvable.

Suppose the $N$ data points $g_i$ have an average station spacing of $\Delta x$. The approximation of the discrete masses $m_k$ to a continuous distribution will be a valid representation of $g$ if the $m_k$ are sufficiently far below the surface relative to $\Delta x$.

Make the average separation of the $N$ masses $\Delta x$ so as to correspond to the average station spacing of $g_i$. Consider the anomaly $g_z\ (x,\ y,\ z)$ at $(x,\ y,\ z)$ resulting from the discrete masses $m_k$ at $(\alpha_k,\ \beta_k,\ h)$

$$g_z(x,\ y,\ z) = K \sum_{k=1}^{N} \frac{m_k(h - z)}{\left\{(x - \alpha_k)^2 + (y - \beta_k)^2 + (z - h)^2\right\}^{3/2}} \cdot \tag{3.4}$$

Taking the Fourier transform of $g_z$ we obtain:

$$G_z(u, v, z) = 2\pi K \exp \left\{ -\frac{h - z}{\Delta x} \sqrt{(u\Delta x)^2 + (v\Delta x)^2} \right\} \times \sum_{k=1}^{N} m_k \epsilon_k, \tag{3.5}$$

where

$$\epsilon_k = \exp(-i\alpha_k u - i\beta_k v)$$

and

$$u = 2\pi f_x; \qquad v = 2\pi f_y,$$

where the $f_x$ and $f_y$ are spatial frequencies measured in cpm in the mks system.

$$\left| \sum m_k \epsilon_k \right| \leq \sum m_k \quad \text{as } \left| \epsilon_k \right| \leq 1. \tag{3.6}$$

Hence $G_z(\beta, v, z)$ is asymptotically dominated by the term

$$\exp \left\{ -\frac{(h - z)}{\Delta x} \cdot \sqrt{[(u\Delta x)^2 + (v\Delta x)^2]} \right\}. \tag{3.7}$$

According to sampling theory (Blackman and Tukey, 1959) the maximum frequency at which $G_z(u, v, z)$ can be specified from the set of values $g_z(x_i, y_i, z_i)$ is the aliasing or folding frequency given by $u_{\max} = \pi/\Delta x$. In fact, in a well-designed survey, the amplitude of $G_z(u, v, z)$ computed from the $g_z$ will approach zero at the aliasing frequency.

Hence, in spectral terms, the discrete equivalent source representation of $g_z$ must also satisfy this requirement. From equation (3.7) $G_z(u, v, z)$ is seen to be negligible at

$$u_{\max} = \pi/\Delta x; \qquad v_{\max} = \pi/\Delta x \tag{3.8}$$

providing $(h-z)/\Delta x$ is sufficiently large. This condition places an upper limit on the plane $z_1$ of the equivalent source.

An effect which places a lower limit on the plane $z_1$ can be deduced from Bullard and Cooper (1948). They noted that the downward continuation of a gravity field, due to a line source, below the source depth induced violent oscillations in the field. As the gravitational intensity and surface contrast density are linked by the equation

$$\sigma(x, y, h) = g_z(x, y, h)/2\pi K,$$

the equivalent source would also experience this effect if placed below the level of a *point or line* source. In the synthetic example following, the depth of the equivalent source was taken at two-thirds the depth of the anomalous gravitating sphere.

In the case of a local survey, its areal extent may also limit the depth of the plane $z_i$. If $(h-z_i)$ is large relative to the dimensions of the survey, the coefficients $a_{ik}$ tend to approach a common value $a$, where

$$\begin{aligned} a &= \lim_{h\to\infty} \frac{(h - z_i)}{\left\{(x_i - \alpha_k)^2 + (y_i - \beta_k)^2 + (z_i - h)^2\right\}^{3/2}} \\ &= \lim_{h\to\infty} 1/(z - h)^2. \end{aligned} \tag{3.9}$$

Thus the matrix $A$ becomes ill-conditioned and its solution unreliable if the equivalent source is too far below the surface; that is if

$$(h - z_i)/\left\{(x_i - \alpha_k)^2 + (y_i - \beta_k)^2\right\}^{1/2}$$

is too large in equation (3.9).

From equation (3.5), a lower limit of $(h-z_i) = 2\Delta x$ gives

$$(u_{\max}, v_{\max}, z) = 2 \times 10^{-4}\; G(0, 0, z) \tag{3.10}$$

sufficient to make $G$ negligible beyond the aliasing frequency.

In a test on part of the data in the case history following, it was found that a value of $(h-z_i) \simeq 5\Delta x$ (Table 1) did not make the matrix $A$ ill-conditioned, demonstrating that the limits on $(h-z_i)$ are sufficiently broad to cover the case of rough topography. Over the entire survey $(h-z_i) \simeq 2.5\Delta x$.

In summary the values $(h-z_i)$ should satisfy

$$2.5\Delta x < (h - z_i) < 6\Delta x, \tag{3.11}$$

where the upper bound is based empirically on the case history.

Equation (3.1) was solved by using Zidarov's application of the "method of steepest descent" which is based on the geometric notion that the equation can be solved by minimizing $R$ with respect to $m_k$.

$$R = (\mathbf{g} - A\mathbf{m})^T(\mathbf{g} - A\mathbf{m}), \tag{3.12}$$

where the superscript $T$ denotes the transpose operator.

This is done by choosing a unit vector $\mathbf{v}$, along the line of maximum change $R$ and along which the initial vector $\mathbf{m}^{(1)}$ is moved a maximum distance $x^{(1)}$ to $\mathbf{m}^{(2)}$. "Distance" is meant in the sense of Ralston (1965, page 44) for a hyperspace of dimension $N$, where $N$ is the number of variables $m_i$.

In general

$$\mathbf{m}^{(j+1)} = \mathbf{m}^{(j)} + \lambda^{(j)}\mathbf{v}^{(j)}. \tag{3.13}$$

Naturally, the reduction of $R$ to zero by $\mathbf{m}^{(j)}$ would give the solution of equation (3.1).

The geometry underlying this method is discussed in the appendix together with the derivation of Zidarov's equation (2). Dropping the superscript $^{(j)}$ we have

$$\lambda = \frac{\sum_{i=1}^{N} f_i \sum_{k=1}^{N} \frac{\partial f_i}{\partial m_k} \frac{\partial R}{\partial m_k}}{\sum_{i=1}^{N}\left(\sum_{k=1}^{N} \frac{\partial f_i}{\partial m_k} \frac{\partial R}{\partial m_k}\right)^2} \tag{3.14}$$

where

$$R = \sum_{i=1}^{N} f_i^2$$

and

$$f_i = g_i - \sum_{k=1}^{N} \frac{m_k(h - z_i)}{\left\{(x_i - \alpha_k)^2 + (y_i - \beta_k)^2 + (z_i - h)^2\right\}^{3/2}} \tag{3.15}$$

where $(x_i, y_i, z_i)$ are the points of measurement and $(\alpha_k, \beta_k, h)$ is the position of $m_k$.

For practical applications the introduction of a factor $a > 1$ into equation (3.13),

$$\mathbf{m}^{(j+1)} = \mathbf{m}^{(j)} + a\lambda^{(j)}\mathbf{v}^{(j)} \tag{3.16}$$

forces the solution through regions in hyperspace where the hyperellipsoid of $R$ becomes very elongated. This makes the method over-relax raising the possibility of a divergent iteration, in which case the iteration is repeated with successively halved values of $a$ until it does converge.

While theoretically it is possible to reduce $R$ to zero, it is more expedient to reduce $R$ to a value at which it is mainly composed of the random errors in $g_i$. As $R$ follows the path of steepest descent in hyperspace, the random errors $\epsilon_i$ of $g_i$ do not influence the gradient $\mathbf{v}_k = \partial R/\partial m_k$ or $\lambda$. In accordance with normal practice (e.g. Kempthorne, 1962, p. 129) assume $\epsilon_i$ normal with mean zero and variance $\sigma$.

$$\frac{\partial R}{\partial m_k} = \sum_{i=1}^{N} 2f_i \frac{\partial f_i}{\partial m_k}$$
$$= 2\sum_{i=1}^{N} \epsilon_i \frac{\partial f_i}{\partial m_k} + 2\sum_{i=1}^{N} f_i^t \frac{\partial f_i}{\partial m_k} \tag{3.17}$$

where

$$f_i^t = g_i^t - \sum_{k=1}^{N} \frac{m_k(h - z_i)}{\left\{(x_i - \alpha_k)^2 + (y_i - \beta_k)^2 + (z_i - h)^2\right\}^{3/2}}$$

and $g_i^t$ is the value of $g_i$ stripped of its random error $\epsilon_i$. That is $g_i = g_i^t + \epsilon_i$, and therefore $f_i = f_i^t + \epsilon_i$. As $(\partial f_i/\partial m_k) < 0$ for all $i$ and $k$, then

$$\sum_{i=1}^{N} 2\epsilon_i \frac{\partial f_i}{\partial m_k} \approx C \sum_{i=1}^{N} \epsilon_i \to 0 \tag{3.18}$$

as $N \to \infty$ from the property that $\epsilon_i$ has a zero mean.

Thus, in the solution of $\mathbf{g} = A\mathbf{m}$, the error criterion $R$ must be reduced until it is less than $E$, the total estimated summed, squared noise in the measurements of $g$. This advantage of the technique in reducing the presence of random errors in the solution of the $m_k$ is passed onto the Bouguer anomaly values later computed from the equivalent source.

$E$ was worked out from

$$R = \sum_{i=1}^{N} f_i^2$$

$$= \sum_{i=1}^{N} (\epsilon_i + f_i^t)^2$$

as $f_i^t \to 0$ while $R \to 0$ despite the influence of the random numbers $\epsilon_i$, therefore $R \to \sum_{i=1}^{N} (\epsilon_i)^2$ as $f_i^t \to 0$.

Thus there is no point in reducing $R$ below the value $N\sigma^2$ where $\sigma$ is the variance of errors. The process of iteration should continue until

$$R < E = N\sigma^2. \qquad (3.19)$$

In developing an algorithm to solve the matrix [equation (3.1)] by the method of steepest descent, the large number of coefficients $a_{ik}$ generated cause computer storage problems. This may be overcome by either storing the values temporarily outside core-storage if sufficient locations are not available or by recomputing the coefficients when required. The latter method was chosen in this case. The algorithm requires $N^2/5000$ sec per iteration on an I.B.M. 360/65 where $N$ is the number of data points. Thus 1000 points would require three minutes per iteration.

Table 1 gives the values of $R$ for successive iterations in analyzing the data discussed in the Case History section below.

The algorithm may be speeded up by improving the initial approximations to $m_k$. The survey is broken up into a number of interconnecting blocks of data sufficiently small so that the matrix which solves for their equivalent source fits within computer core storage. This vastly increases algorithm efficiency as the operation of recalculating coefficients is not required. For example, the equivalent source of 100 points can be calculated in less than a second per iteration on the 360/65. The values of the $m_k$ found for the individual blocks can then be put together as the initial values of the equivalent source for the entire survey.

## SYNTHETIC TEST

The technique was tested on synthetic data. The gravity field of a sphere at a depth of 100 units was computed at points 25 units apart over an idealized terrain representing a valley and plateau separated by a 25 unit high cliff (Figure 1A). This field is contoured in Figure 1B.

**Table 1. The numerical convergence of $R$ using the steepest descent procedure**

| | Value of $R=\sum_{i=1}^{N}(g_i-g_i^{(j)})$ | Iteration cycle ($j$) | Convergence? |
|---|---|---|---|
| a) Derby-Winnaleah Area $(h-z_i)\approx 2.5\Delta x$ | | | |
| | 3887.459 | 1 | yes |
| | 1562.7364 | 2 | yes |
| | 1063.3290 | 3 | yes |
| | 739.07411 | 4 | yes |
| Note slow convergence | 556.31239 | 5 | yes |
| | 556.31232 | 6 | yes |
| Region of nonconvergence | 2896.7126 | 7 | no |
| | 556.31234 | 8 | no |
| Note fast convergence | 263.76229 | 9 | yes |
| | 139.69104 | 10 | yes |
| | 86.758592 | 11 | yes |
| | 59.154730 | 12 | yes |
| | 44.441891 | 13 | yes |
| b) Test Area $(h-z_i)\approx 5.0\Delta x$ | | | |
| | 1197.9390 | 1 | yes |
| | 384.77229 | 2 | yes |
| | 214.14105 | 3 | yes |
| | 118.76362 | 4 | yes |
| Note slow convergence | 84.163410 | 5 | yes |
| | 84.163409 | 6 | yes |
| Region of nonconvergence | 467.92798 | 7 | no |
| | 84.163406 | 8 | yes |
| | 84.163423 | 9 | no |
| Note fast convergence | 30.586830 | 10 | yes |
| | 19.190139 | 11 | yes |

Figure 1C compares the theoretically correct field and the field projected from the terrain surface values to a common datum plane by use of the equivalent source technique.

The difference between the two fields, which is the error of the projected field, is plotted in Figure 1C. The maximum absolute error, which is seen to occur over the sphere, represents a relative error of only three percent.

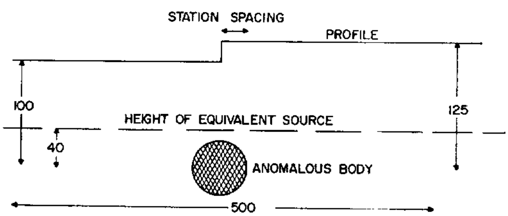


FIG. 1A. The synthetic test of an anomalous gravitating body and terrain.

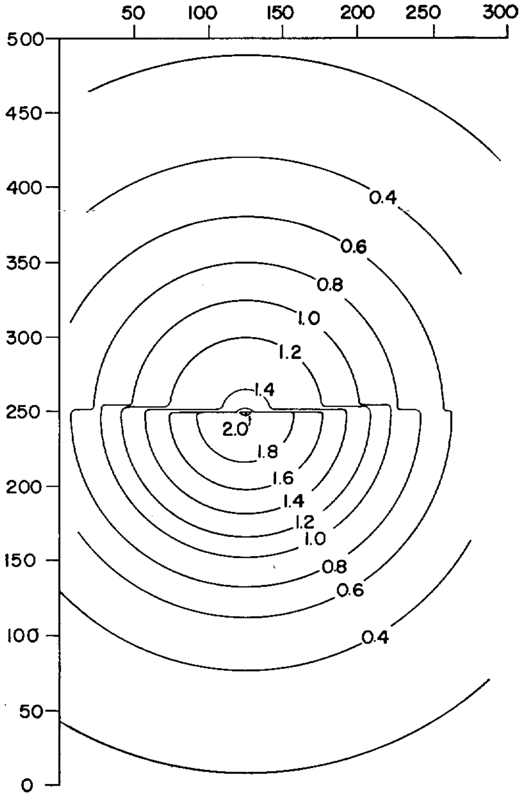


FIG. 1B. The Bouguer anomaly measured over the terrain of Figure 1A. Contour values in mgal.

### CASE HISTORY—THE DERBY WINNALEAH GRAVITY SURVEY

The equivalent source technique was tested on data collected by Howland-Rose (1966) on behalf of the Australian Commonwealth Bureau of Mineral Resources at Derby, Tasmania, Australia. The location of the survey is shown in Figure 2.

The survey of about 4 sq mi was chosen for this study as its area is extremely precipitous due to the influence of the Ringarooma River on the topography.

The geology of the Ringarooma Valley, which includes the survey area, has been described by Nye (1925) (Figure 3).

The oldest rock in the area is the Silurian Mathinna Group composed of slates and sandstones. During the course of geological time this group has been extensively folded and faulted.

During the Devonian, the Mathinna Group suffered its most extensive period of diastrophism. It was extensively intruded and folded by granite to form hills which rose out of the pre-Tertiary landscape. A long period of erosion which followed the granite intrusions, cut deeply into the topography. Veins in the granite were leached of tin which was subsequently deposited as low density (2.0 gm/cm$^2$) alluvium along depressions in the plane levelled out of the Mathinna Sandstone.

The topography at the beginning of the Tertiary had thus been formed by the eroding influence of the Ringarooma River. The river's path was controlled by the resistant hills of granite and sandstone, and by a relative depression in the land surface to the nearby sea which lowered the river's slope, changing it to a series of small lakes and estuaries.

Then, during the Tertiary, this quiescent scene was disrupted by the outpourings of basaltic lava flows. The Ringarooma River channel was

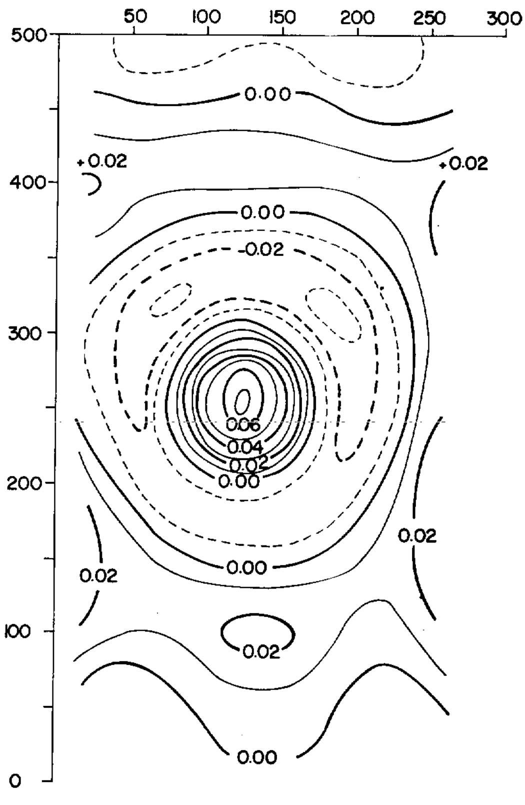


FIG. 1C. The absolute errors of the Bouguer anomaly values projected from Figure 1B using the equivalent source technique. Dashed contours represent negative errors. Contour interval = 0.01 mgal.

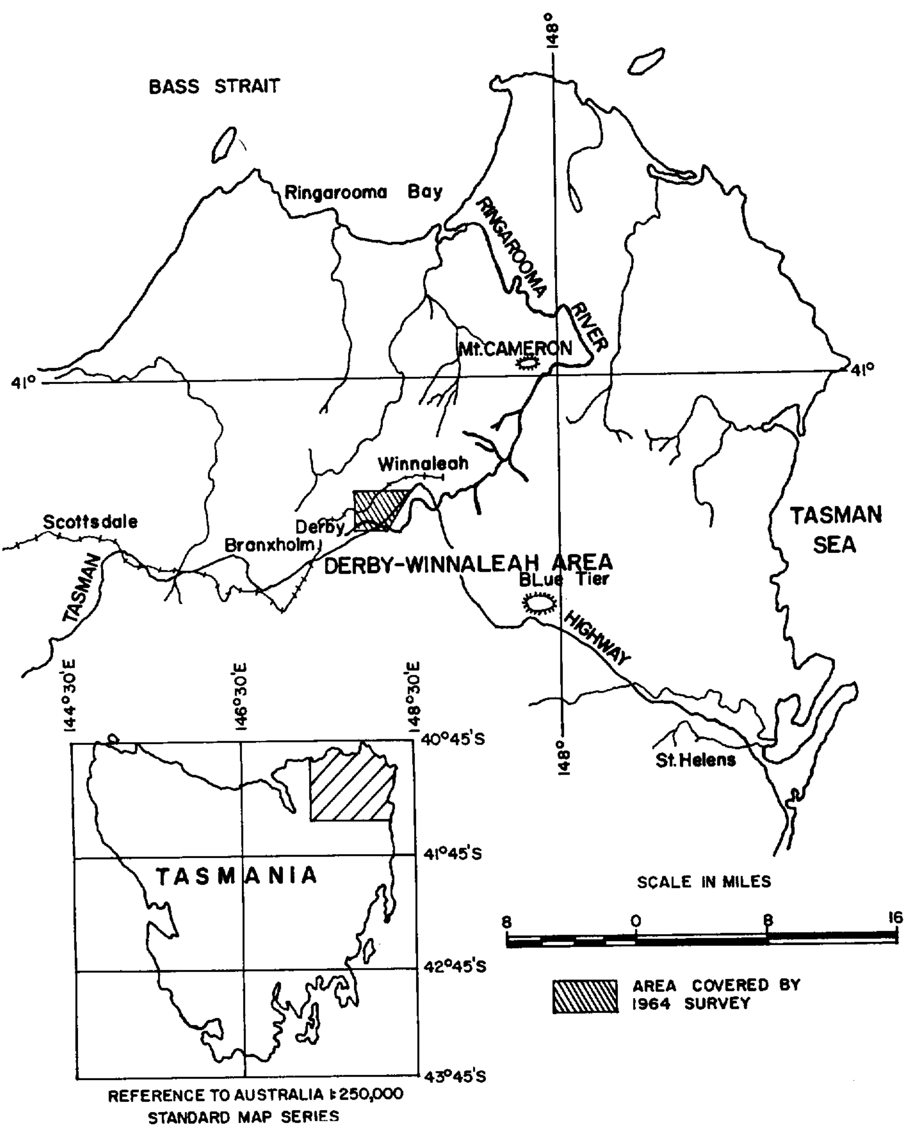


FIG. 2. Derby-Winnaleah area, Tasmania, locality map.

buried by lava and its course changed at Derby as it was forced along the granite basaltic lava contact in the survey area. The ancient river that had previously flowed west of the Mt. Cameron Range (Figure 2) was diverted to the east.

The modern Ringarooma River has eroded its way down the gorge now containing the Briseis Mine (Figure 3) in the survey area. A rough north-south cross section is shown in Figure 4 of a simplified interpretation of the area's geology.

The gravity observations were reduced in a manner following Hammer (1963) so that the final topographically corrected Bouguer anomalies took into account the simple model of the geology shown (see cross section) down to 150 m above mean sea level ("base" level in Figure 4). Bott's (1961) method for calculating the topographic effect was employed. The topographic correction was defined as in Grant and West (1965, p. 239) and hence, following Bott, the various densities of the rocks were used to compute the topographic correction. The Bouguer

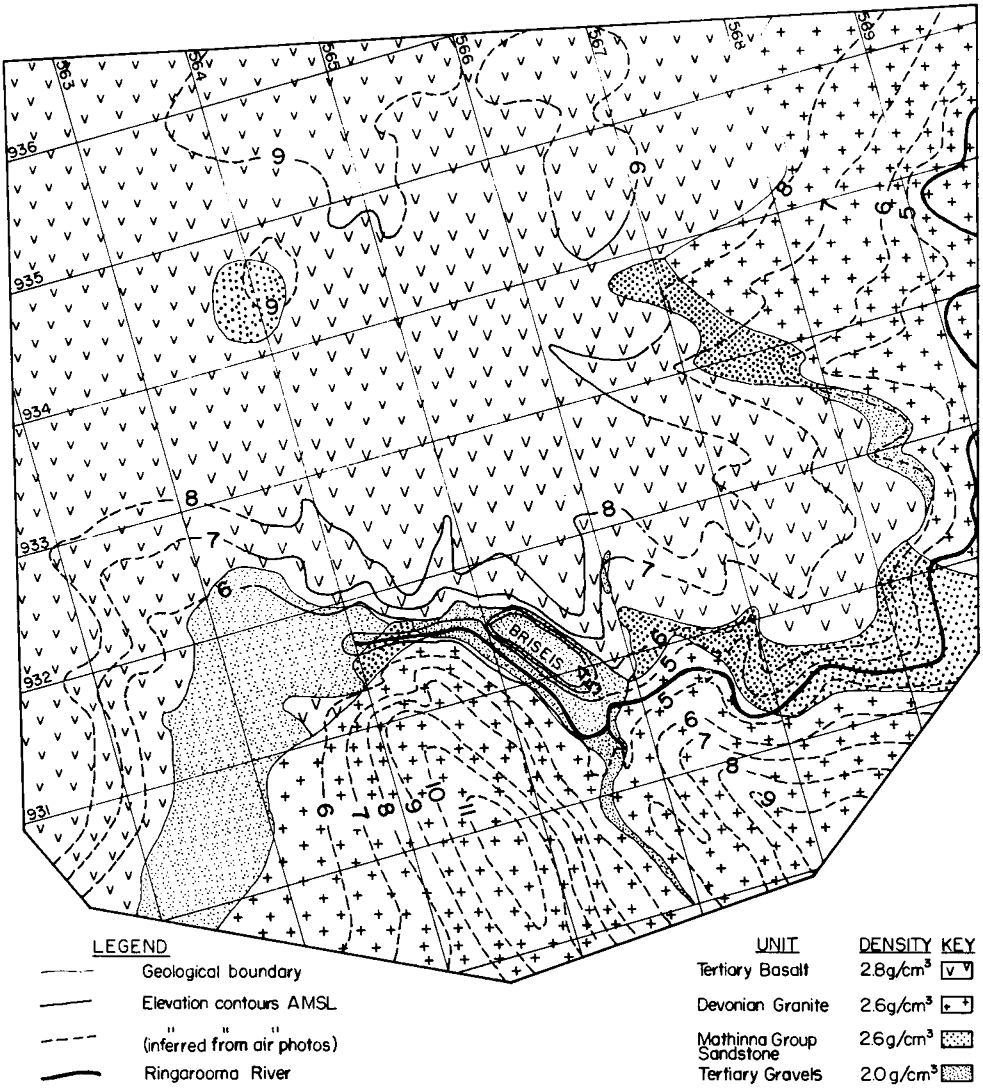


Fig. 3. Geology and topography of Derby. Elevation values are in units of 100 ft. Northings and Eastings are in units of 1000 yards.

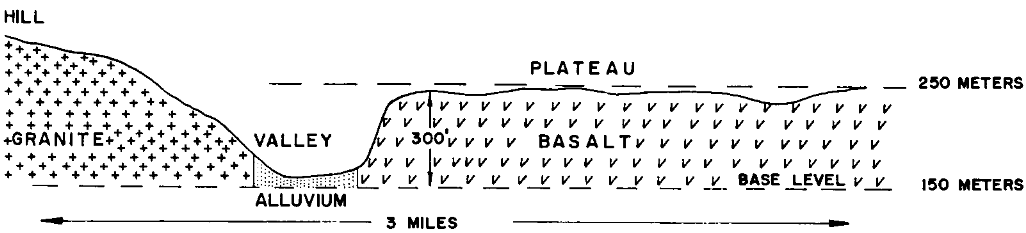


Fig. 4. Diagrammatic cross section through plateau and valley, north to south. All heights are with reference to mean sea level.

anomalies are shown in Figure 5. As absolute Bouguer anomaly values are not required in a local survey, the zero contour has been set so that it passes through the center of the map.

The equivalent source of this Bouguer anomaly map was found. The noise level parameter $E$ was worked out from equation (3.19) to be 50 $(\text{mgal})^2$ for the 860 stations involved. The random error of each Bouguer anomaly value was taken to be the order of 0.25 mgal. This is reasonable in view of the precipitous topography and the associated difficulty of making exact topographic corrections. The plane of the equivalent source was taken at a height equal to mean sea level which satisfies the previously discussed limits.

The Bouguer anomalies at regular grid points on a horizontal plane about the same height as the basalt plateau (250 m $\approx$ 800 ft) were then computed from the equivalent source and are plotted in Figure 6. The grid itself is not shown, but it has

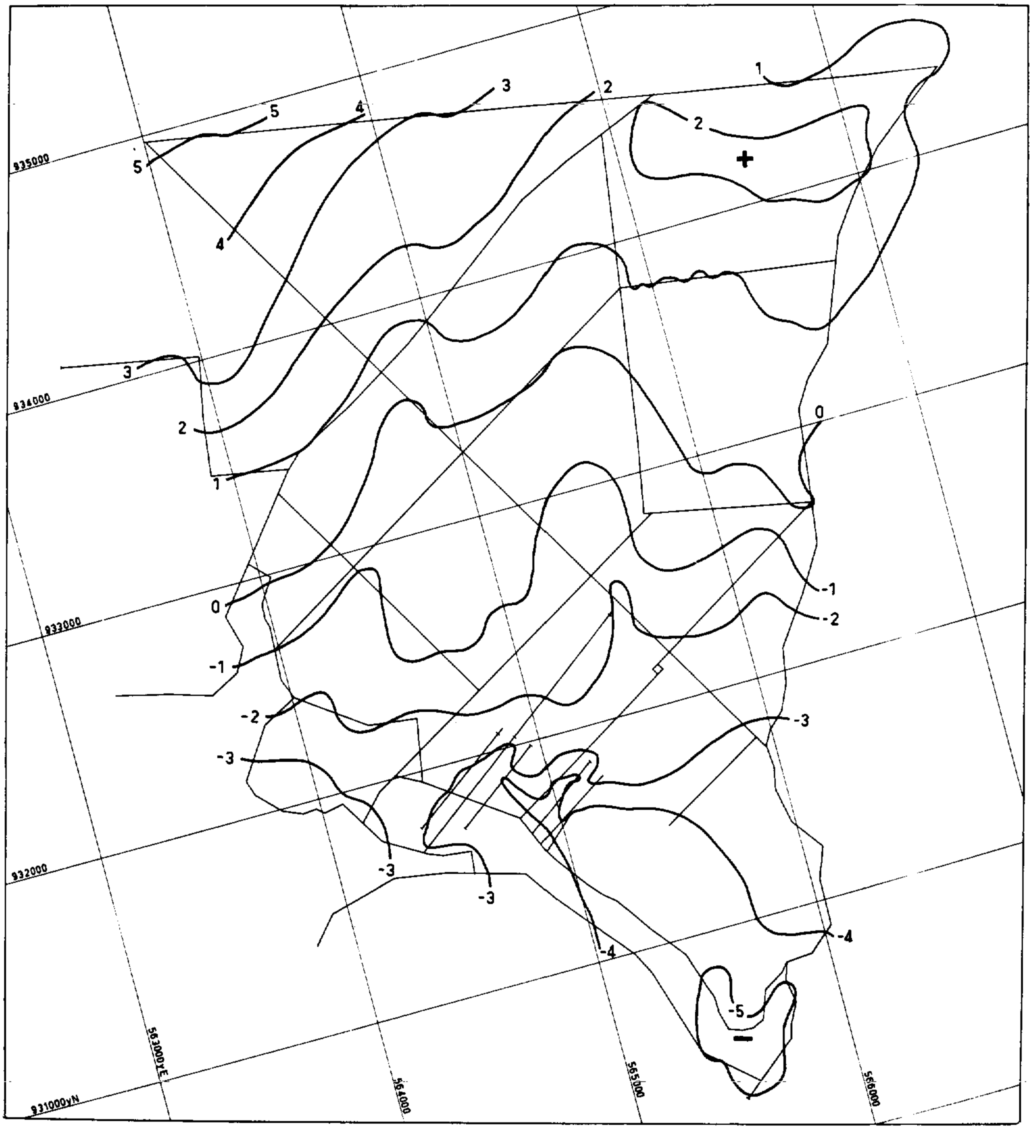


FIG. 5. Topographically corrected Bouguer anomalies for the Derby-Winnaleah area. Contour interval = 1.0 mgal.

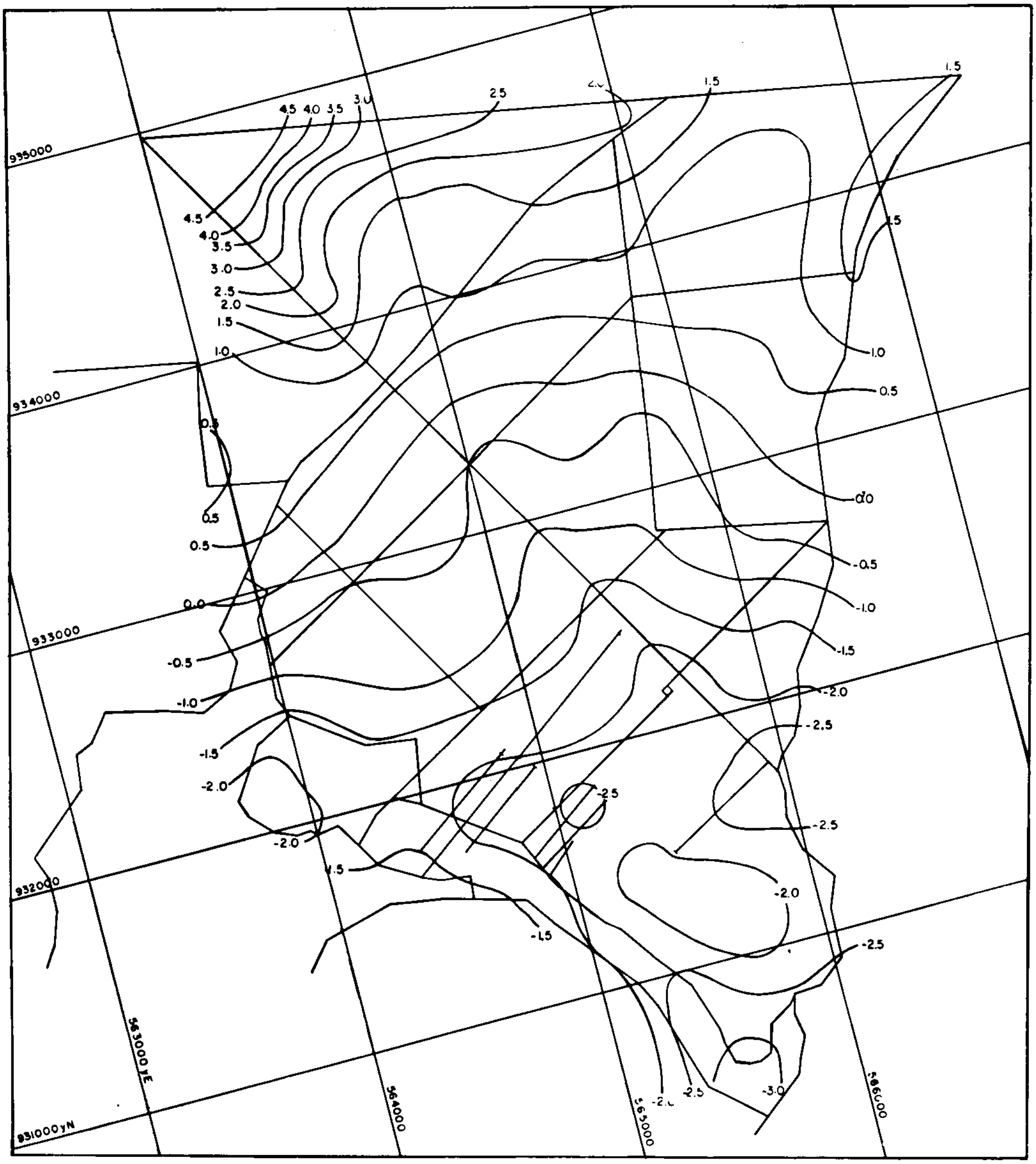


FIG. 6. The topographically corrected Bouguer anomalies at 250 m above mean sea level. Contour interval = 0.5 mgal.

a mesh interval of 100 m and extends over the area contoured. Comparison of Figures 5 and 6 shows that the technique's projection of the original Bouguer anomaly values has eliminated minor random fluctuations present in the contours of Figure 5. Projection of the values in the valley region (delimited to the North by the −3.0 contour in Figure 5) to the same reference plane as the plateau values, allows a direct comparison of the Bouguer anomalies across the 300 ft elevation difference between the two regions. Evenly spaced grid points also allow more objective contouring than do long survey lines.

The Bouguer anomalies are now in a satisfactory form for processing by techniques requiring gridded data.

However, the simplicity of directly calculating the field from the equivalent source suggests using the technique for vertical continuation. Figure 7 shows the dominant regional trend of the Bouguer anomalies, computed in this way, on a plane 500 m above sea level.

The final residual map, Figure 8, was found by subtracting the "regional" values (defined by Figure 7) from the values at 250 m (Figure 6). The major negative trend across the map apparently reveals the low density alluvium marking the buried channel of the ancient Ringarooma River. The positive anomaly in the southeast corner is attributed to the water filled Briseis mine workings taken as being empty in the topographic corrections. The two positive anomalies in the northeast and northwest corners, corresponding to Mathinna sandstone outcrops, mark the limits


FIG. 7. The topographically corrected Bouguer anomalies at 500 m above mean sea level. Contour interval = 0.5 mgal.

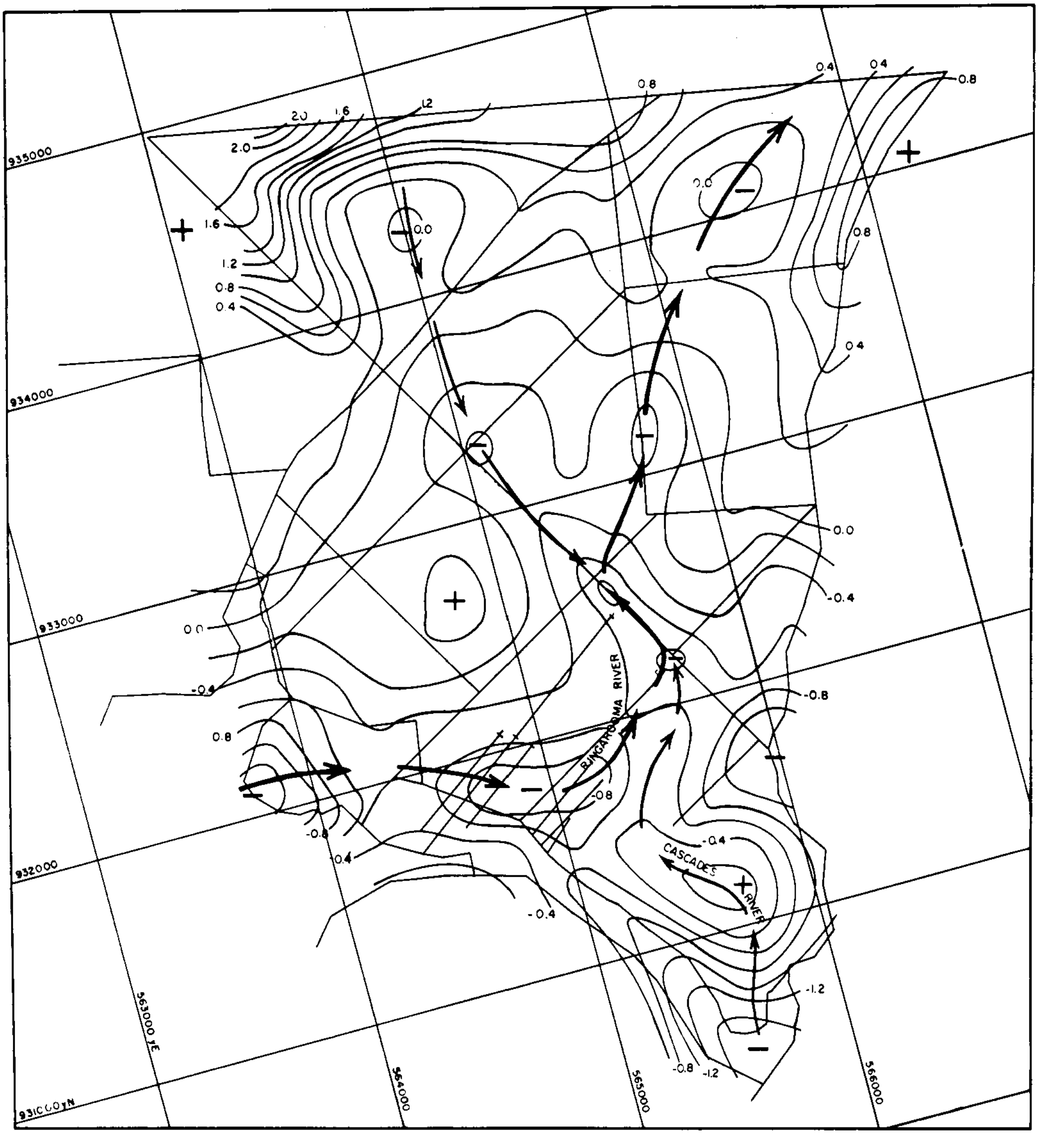


FIG. 8. The topographically corrected residual Bouguer anomalies at 250 m above mean sea level. Contour interval = 0.2 mgal.

of the alluvial plane imposed by these resistant pre-Tertiary hills of sandstone and granite.

## CONCLUSION

The equivalent source technique as demonstrated in Synthetic Test section and the Case History offers a convenient and accurate way to interpolate gravity data onto a grid. It can be used to make the final correction to the Bouguer anomaly by projecting measurements onto a horizontal reference plane. The technique has the important application of objective preparation of Bouguer anomalies for processing by methods mentioned in the review. It should also be possible easily to extend this technique to other potential fields, particularly magnetic fields.

However, limitations have to be realized. Projecting gravity data onto a horizontal plane involves vertical continuation and so a large horizontal coverage of field values may be required.

This can be seen from the lateral extent of the theoretically perfect coefficient set for vertically continuing a potential field at a height equal to the station spacing. (Dampney, 1966a).

This technique offers a low-error-level, objective approach to three-dimensional interpolation and the related problem of contouring data. As an added bonus it is very economical to use the equivalent source (once calculated) for reasonably accurate vertical continuation.


## ACKNOWLEDGEMENTS

This research formed part of an M.Sc thesis program carried out in the Department of Geology, University of Tasmania (Dampney, 1966b). I gratefully acknowledge the help and inspiring supervision of Dr. R. Green.

Sincere thanks are extended to Dr. G. F. West, Geophysics Laboratories, University of Toronto, for his useful comments made during the preparation of this manuscript.

The author is also indebted to Mr. J. Boothroyd for programming advice and to the Director, Australian Commonwealth Bureau of Mineral Resources for permission to publish the Derby Winnaleah Case History.


## REFERENCES


Bhattacharyya, B. K., 1965, Two-dimensional harmonic analysis as a tool to magnetic interpretation: Geophysics, v. 30, p. 829–857.

——— 1966, Continuous spectrum of the total magnetic field anomaly due to a rectangular prismatic body: Geophysics, v. 31, p. 97–121.

Blackman, R. B., and Tukey, J. W., 1959, The measurement of power spectra: New York, Dover Publications, Inc.

Bott, M. H. P., 1961, The use of electronic digital computers for the evaluation of gravimetric terrain corrections: Geophys. Prosp., v. 7, p. 45–54.

——— 1967, Solution of the linear inverse problem in magnetic interpretation with applications to oceanic magnetic anomalies: Geophys J. R. Astr. Soc., v. 12, p. 151–162.

Bullard, E. C., and Cooper, R. I. B., 1948, The determination of the masses necessary to produce a given gravitational field: Proc. Roy. Soc. (London) Ser. A., v. 194, p. 332–347.

Dampney, C. N. G., 1966a, Three criteria for the judgement of vertical continuation and derivative methods of geophysical interpretation: Geoexploration, v. 4. p. 3–24.

——— 1966b, Geophysical studies in Tasmania; Part A, Interpretation of the gravitational potential field using the frequency domain: M.Sc. Thesis (unpubl.), Dept. of Geology, Univ. of Tasmania.

Daneš, Z. F., 1961, Structure calculations from gravity data and density logs: Mining Trans, v. 223, p. 23–29.

Grant, F. S., and West, G. F., 1965, Interpretation theory in applied geophysics: New York, McGraw-Hill Book Co., Inc.

Hammer, S., 1963, Deep gravity interpretation by stripping: Geophysics, v. 28, p. 369–378.

Henderson, R. G., 1960, Comprehensive system of automatic computation in magnetic and gravity measurements: Geophysics, v. 25, p. 564–585.

Howland-Rose, A., 1966, Derby-Winnaleah Survey, Tasmania 1964: Dept. of National Development, Bureau of Mineral Resources, Geology and Geophysics, Record No. 1966/10.

Kempthorne, O., 1962, Design and analysis of experiment: New York, John Wiley and Son.

Naudy, H., and Neumann, R., 1965, Sur la définition de l'anomalie de Bouguer et ses conséquences pratiques: Geophys. Prosp., v. 13, p. 1–11.

Neidell, N. S., 1966, Spectral studies of marine geophysical profiles: Geophysics, v. 31, p. 122–134.

Nye, P., 1925, The sub-basaltic tin deposits of the Ringarooma Valley: Tas. Dept. of Mines, Geological Survey Bull. No. 35.

Ralston, A., 1965, A first course on numerical analysis: New York, McGraw-Hill Book Co. Inc.

Roy, A., 1962, Ambiguity in geophysical interpretation: Geophysics, v. 27, p. 90–99.

Sax, R. L., 1966, Applications of filter theory and information theory to the interpretation of gravity measurements: Geophysics, v. 31, p. 570–575.

Strakhov, V. N., and Devitsyn, V. M., 1965, The reduction of observed values of a potential field to values at a constant level: Bull. Acad. Sci. USSR., Geophys. Ser. (English Transl.), p. 250–255.

Zidarov, D., 1960, Détermination des champs de gravitation (ou magnétiques) locaux et régionaux: Comptes rendus de l'Académie bulgare des Sciences, v. 13, p. 531–534.

——— 1965, Solutions of some inverse problems of applied geophysics: Geophys. Prosp., v. 13, p. 240–246.


## APPENDIX

*Derivation of equation (3.12)*

$$\text{Minimize } R = (\mathbf{g} - A\mathbf{m})^T(\mathbf{g} - A\mathbf{m}) \quad (1)$$

to find the solution of $\mathbf{m}$ in equation (3.12). The direction of maximum change of $R$ with respect to $m_i$ is given by $\partial R/\partial m_i$ the $i$th component of $\nabla R$ with respect to $m$.

Thus following Zidarov (1965)

$$R = \sum_{i=1}^{N} \left\{ g_i(M_k) - g_i^{(j)}(m_k) \right\}, \quad (2)$$

$$g_i^{(j)} = \sum_{k=1}^{N} m_k^{(j)} \frac{(h - z_i)}{\left\{(x_i - \alpha_k)^2 + (y_i - \beta_k)^2 + (z_i - h)^2\right\}^{3/2}}, \quad (3)$$

$g_i(M_k)$ is the measured field due to the true masses $M_k$, and $g_i^j\ (m_k)$ is the $j$th approximation of $g_i$ from the approximate masses $m_k^{(j)}$ at $(\alpha_k, \beta_k, h)$.

The positions of the $m_k$ are not restricted, but for convenience place all the $m_k$ at the same height. In the case history, each discrete mass was positioned vertically below each of the $N$ data points making up the survey. However, any other arrangement is valid within restrictions imposed by equation (3.12) and the nature of the matrix $A$. In the solution we assume nothing about the elements of $A$ except that they are real and that $A$ is square.

Therefore,

$$\frac{\partial R}{\partial m_i} = \sum_{k=1}^{N} 2f_k \frac{\partial f_k}{\partial m_i} \tag{4}$$

where

$$_k = g_k(M_i) - \sum_{i=1}^{N} \cdot \frac{m_i(h - z_k)}{\{(x_k - \alpha_i)^2 + (y_k - \beta_i)^2 + (z_k - h)^2\}^{3/2}},$$

that is

$$R = \sum_{i=1}^{N} f_i^2. \tag{5}$$

We find following equation (3.11) that

$$m_k^{(j)} = m_k^{(j-1)} - \lambda^{(j-1)} \frac{\partial R}{\partial m_k^{(j-1)}} \tag{6}$$

where $m_k^{(j)}$ is a closer approximation to the true value of $m_k$ than $m_k^{(j-1)}$.

Therefore,

$$R = R\left(m_1^{(j)} - \lambda^{(j)} \frac{\partial R}{\partial m^{(j)}}, \cdots, m_N^{(j)} - \lambda^{(j)} \frac{\partial R}{\partial m_N^{(j)}}\right)$$

is less than $R = R(m_1^{(j)}, \cdots, m_N^{(j)})$.

To reduce $R$ as quickly as possible, we maximize $\phi(\lambda)$ with respect to $\lambda$:

$$\phi(\lambda) = R\left(m_1^{(j)} - \lambda^{(j)} \frac{\partial R}{\partial m_1^{(j)}}, \cdots, m_N^{(j)} - \lambda^{(j)} \frac{\partial R}{\partial m_N^{(j)}}\right). \tag{7}$$

Developing $\phi(\lambda)$ as a power series in $\lambda$ from Taylor's theorem, and taking into consideration only the first two terms (as $d^3R/\partial m_k^3 = 0$ for all $k$ from equation 4), we obtain

$$\phi(\lambda) = R - \lambda \frac{dR}{d\mathbf{m}} \frac{dR}{d\mathbf{m}} + \frac{\lambda^2}{2!}\left(\frac{dR}{d\mathbf{m}}\right)^2 \frac{d^2R}{d\mathbf{m}^2}. \tag{8}$$

$$\frac{d^2R}{d\mathbf{m}^2} = 2\left(\frac{df}{d\mathbf{m}}\right)^2 + 2\mathbf{f}\frac{d^2\mathbf{f}}{d\mathbf{m}^2}. \tag{9}$$

Now $d^2f/d\mathbf{m}^2 = 0$ from equation (4), therefore

$$\phi(\lambda) = \mathbf{f}^2 - 4\lambda\mathbf{f}^2\left(\frac{d\mathbf{f}}{d\mathbf{m}}\right)^2 + 4\lambda^2\mathbf{f}^2\left(\frac{d\mathbf{f}}{d\mathbf{m}}\right)^4; \tag{10}$$

$\phi(\lambda)$ will have a maximum when $d\phi/d\lambda = 0$. Thus

$$4\mathbf{f}^2\left(\frac{d\mathbf{f}}{d\mathbf{m}}\right)^2 - 8\lambda\mathbf{f}^2\left(\frac{d\mathbf{f}}{d\mathbf{m}}\right)^4 = 0. \tag{11}$$

Hence

$$\begin{aligned}\lambda &= \mathbf{f}^2\left(\frac{d\mathbf{f}}{d\mathbf{m}}\right)^2 \Big/ 2\mathbf{f}^2\left(\frac{d\mathbf{f}}{d\mathbf{m}}\right)^4 \\ &= \mathbf{f}\frac{d\mathbf{f}}{d\mathbf{m}}\frac{dR}{d\mathbf{m}} \Big/ \left(\frac{d\mathbf{f}}{d\mathbf{m}}\right)^2\left(\frac{dR}{d\mathbf{m}}\right)^2 \\ &= \frac{\sum_{i=1}^{N} f_i \sum_{k=1}^{N} \frac{\partial f_i}{\partial m_k}\frac{\partial R}{\partial m_k}}{\sum_{i=1}^{N}\left(\sum_{k=1}^{N}\frac{\partial f_i}{\partial m_k}\frac{\partial R}{\partial m_k}\right)^2}\end{aligned} \tag{12}$$

which is Zidarov's (1965) equation (2) with $m_k$ substituted for $\theta_{jk}$ and $R$ for $U$.

This method assumes $R$ has only one minimum. The condition for one minimum that $d^3R/d\mathbf{m}^3 = 0$ is seen to be true.

### *Geometric considerations*

Ralston (1965, p. 439–442) derives an equation for $\lambda$ for the case of a symmetric matrix. He also discusses the geometry of the method of steepest descent.

The geometry for the unsymmetric matrix is similar. For ideal convergence the magnitude of

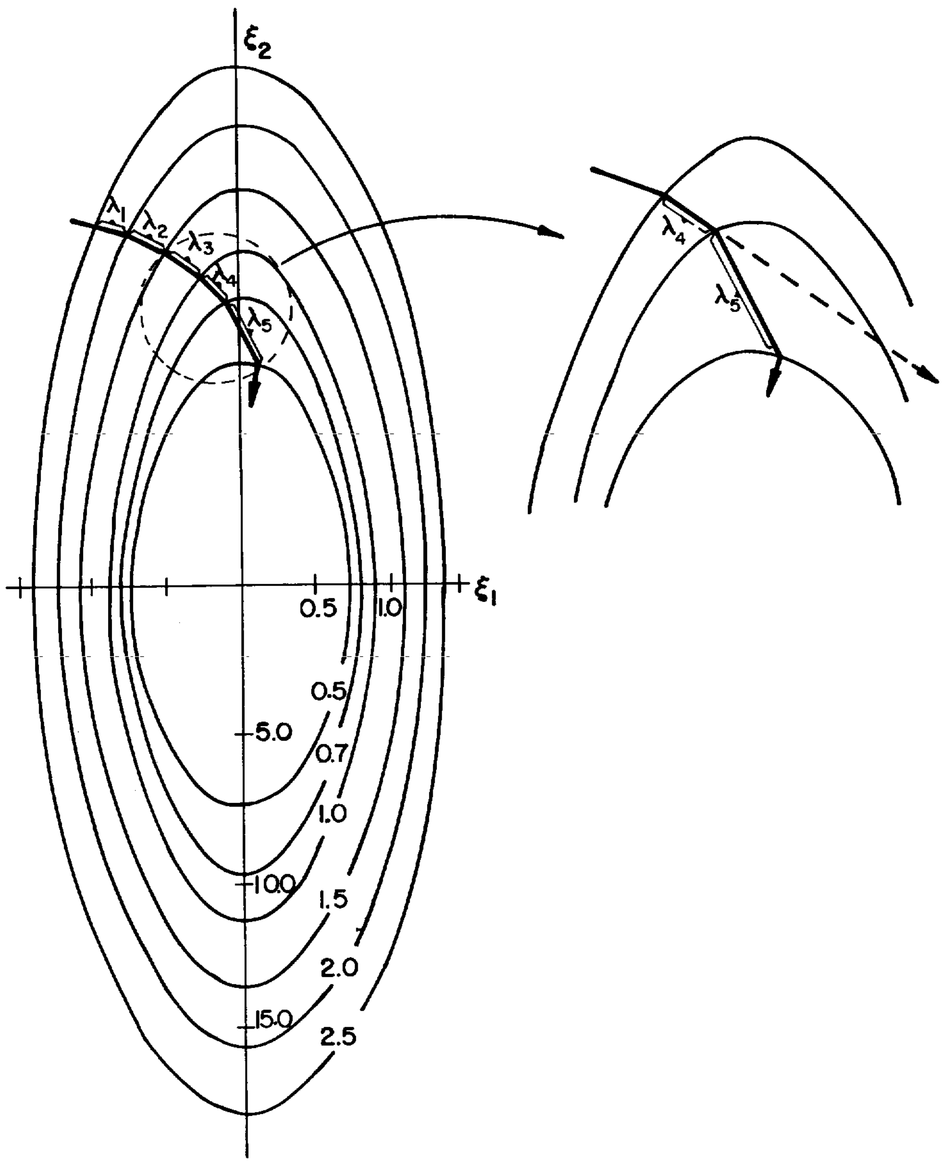


FIG. 9. The path of the steepest descent solution.

the successive iterations $\lambda^{(1)}$, $\lambda^{(2)} \cdots$ from the first approximation is shown in Figure 9.

$$\boldsymbol{\varepsilon} = \mathbf{g} - A\mathbf{m}$$

in the figure and $\boldsymbol{\xi}$ represents the major and minor axes of the hyperellipsoid $R$.

Physically one sees in the solution of $\mathbf{g} = A\mathbf{m}$ that if the true value of $m_k$ is greatly different from the other $m$'s, the hyperellipsoid is very elongated along the $m_k$ axis. This may result if $m_k$ is in a position where the actual source is small and shallow and the effect described by Bullard and Cooper (1948) discussed in section 3 occurs.

As the solution will work its way towards elongated regions of the hyperellipsoid, the influence of small (relative to the station spacing) shallow sources will be the last to be extracted from $R$. Hence as $R$ is not reduced to zero, the shallow sources will be treated as noise in the data. As small shallow sources are by definition inadequately sampled, their elimination as noise is in accordance with normal practice.